DYNAMIC CELL ADHESION AND MIGRATION ON NANOSCALE GROOVED SUBSTRATES

E. Lamers[1†], J. te Riet[2†], M. Domanski[3], R. Luttge[3], C.G. Figdor[2], J.G.E. Gardeniers[3], X.F. Walboomers[1] and J.A. Jansen[1*]

[1] Department of Biomaterials, Radboud University Nijmegen Medical Centre, Nijmegen, The Netherlands
[2] Department of Tumor Immunology, Nijmegen Centre for Molecular Life Sciences, Radboud University Nijmegen Medical Centre, Nijmegen, The Netherlands
[3] MESA Institute for Nanotechnology, University of Twente, Enschede, The Netherlands
[†] Contributed equally to this work

Abstract

Organised nanotopography mimicking the natural extracellular matrix can be used to control morphology, cell motility, and differentiation. However, it is still unknown how specific cell types react with specific patterns. Both initial adhesion and preferential cell migration may be important to initiate and increase cell locomotion and coverage with cells, and thus achieve an enhanced wound healing response around an implantable material. Therefore, the aim of this study was to evaluate how MC3T3-E1 osteoblast initial adhesion and directional migration are influenced by nanogrooves with pitches ranging from 150 nm up to 1000 nm. In this study, we used a multi-patterned substrate with five different groove patterns and a smooth area with either a concentric or radial orientation. Initial cell adhesion measurements after 10 s were performed using atomic force spectroscopy-assisted single-cell force spectroscopy, and demonstrated that nascent cell adhesion was highly induced by a 600 nm pitch and reduced by a 150 nm pitch. Addition of RGD peptide significantly reduced adhesion, indicating that integrins and cell adhesive proteins (e.g. fibronectin or vitronectin) are key factors in specific cell adhesion on nanogrooved substrates. Also, cell migration was highly dependent on the groove pitch; the highest directional migration parallel to the grooves was observed on a 600 nm pitch, whereas a 150 nm pitch restrained directional cell migration. From this study, we conclude that grooves with a pitch of 600 nm may be favourable to enhance fast wound closure, thereby promoting tissue regeneration.

Keywords: Cell-protein-material interactions, tissue-material interactions, biomaterials, nanotechnology, imaging, AFM profilometry, cells motility, cell migration, tissue adhesion.

* Address for correspondence:
John A. Jansen, DDS, PhD
Department of Biomaterials
Radboud University Nijmegen Medical Centre 309 PB
PO Box 9101, 6500HB Nijmegen
The Netherlands

Tel: +31 24 3614920
Fax: +31 24 3614657
E-mail:j.jansen@dent.umcn.nl

Introduction

The natural extracellular matrix (ECM) of living tissues is a complex system, highly organised at the macro-, micro-, and nanoscale. Hence, cells are continuously subjected to nanotopographical cues mediated by the cells' integrins and ECM adhesion proteins. Collagen type I in bone, for example, forms fibrils with a typical banding pattern of 68 nm in width with a 3-5 nm banding depth and a 35 nm interfibrillar spacing depth (Weiner and Wagner, 1998). By interacting with their natural nano environment, cells become activated and differentiate to perform their intended function (Biggs *et al.*, 2009; Dalby *et al.*, 2007; Dang and Leong, 2007; Lamers *et al.*, 2010a; Yim *et al.*, 2007). Nowadays in tissue engineering and regenerative medicine, much effort is placed in mimicking such nanotopography on implantable biomaterials. Cells possibly recognise such topographies as a more "natural" environment, leading to fast integration of the biomaterial into the surrounding tissue (Lamers *et al.*, 2010a; Pierres *et al.*, 2002).

In addition to cellular differentiation, using an organised topography on implantable materials will also control the morphological and migration behaviour of cells. The latter may be employed to achieve a fast closure of the wound area over an implant surface, thereby shortening the healing time and preventing the occurrence of infections. For example, in guided tissue regeneration (GTR), membranes consisting of a highly organised array of collagen are implanted to promote fast, directional migration of cells (Behring *et al.*, 2008). Our previous study demonstrated that cell motility and morphology are highly influenced by differences in groove dimensions (Lamers *et al.*, 2010b). On grooves with specifically a width of 300 nm, for example, cells aligned to the groove direction and were highly motile, indicating a favourable response for GTR. On the other hand, we could not observe any motility and morphological effects on grooves narrower than 75 nm, irrespective of the applied groove depth or ridge width. Despite the studies on the influence of cellular behaviour to a wide array of nanogrooved dimensions, it is thus far unknown how specific cell types react with specific patterns. In addition, it is unknown how cell adhesive processes are involved in such directional cell migration.

To understand how cellular responses towards biomaterial structures are mediated, cell adhesion needs to be studied in detail. The initiation of cell adhesion

is a process which is usually established within a few microseconds (Carvalho *et al.*, 2010) and involves integrins that adhere to surface specific proteins such as fibronectin and vitronectin (Pierres *et al.*, 2008; Siebers *et al.*, 2005). Within 5 min, these integrins cluster to become focal adhesions (FAs), and may either disassemble or further mature into fibrillar adhesions (FBs) within 20 min (Gardel *et al.*, 2010; Zaidel-Bar *et al.*, 2003). The formation of such FBs may severely reduce cell motility (Coussen *et al.*, 2002), as shown in our previous study (Lamers *et al.*, 2010b). Such cell adhesive processes are not only important for proper integration of an implant into the surrounding tissue, but likely also influence other cellular processes such as migration, polarisation, spreading, and differentiation. Therefore, the aim of this study was to get a better understanding of the effect of nanoscale grooves on initial osteoblast adhesion within the first hour after the cells come into contact with the surface, and how this adhesion can be related to directional cell migration on the grooves.

We hypothesise that a fast adhesion of cells to grooved implants leads to increased directional migration. Ultimately, this may result in improved wound healing and tissue regeneration not only in an outside-in fashion but also at the inner surface of an implant shortly after implantation. In order to test this hypothesis, different types of cell adhesion studies were performed. The influence of nanoscale grooves ranging from a pitch of 150 nm up to 1000 nm was first studied directly after initial contact using atomic force microscopy (AFM) single cell force measurements. Next, initial cell adhesion events were followed at intervals from minutes to hours. Finally, a migration assay up to three days was performed to assess whether the initial adhesion correlated to the tissue migration potential of osteoblasts after prolonged culture.

Materials and Methods

Substrates

Prime quality 4'' silicon (Si) wafers with nanogrooves were prepared using laser interference lithography (Lamers *et al.*, 2010a). A setup was used based on the Lloyd's interferometer, where a regular pattern was produced by interference of an incident laser beam and a mirror reflected beam (van Soest *et al.*, 2005). The period of the interference pattern, and thus of the grating recorded in the resist layer on the substrate, is given by the equation: $P = \lambda/(2\sin\theta)$, where the period (P) is determined by the wavelength (λ) of the beam source and the angle (θ) at which two coherent beams are interfering. With a 266 nm light source, periods of 150 nm up to 1000 nm were produced (Luttge, 2009). A tri-layer positive resist system was spin-coated on a silicon wafer, consisting of a 13 nm thick bottom antireflective coating (BARC) DUV46 (Brewer Science, Derby, UK), a 140 nm thick positive (for PS replication) photosensitive polyvinyl-based resist PEK500 (Sumitomo Chemical, Tokyo, Japan), and a 5 nm top antireflective coating (TARC, Aquatar-6A, AZ Electronics, Wiesbaden, Germany). After illumination and development of the resist layer, the grating was transferred to the substrate by a reactive ion etching process using a Plasmatherm 790 system (Unaxis, Utrecht, The Netherlands). An optimised method of reactive ion etching using parameters giving anisotropic etch profiles in nanoscale was used. SF_6:O_2 plasma chemistry gave well defined structures transferred into the silicon substrate. Using this setup, highly regular patterns were produced over areas of about 2 x 2 cm^2. The groove dimensions are given in Fig. 1a.

In order to create multi-patterned wafers containing 5 different groove patterns and 1 flat part, five Si wafers containing different groove patterns and one smooth substrate were diced into sextant pieces and glued together to create one combined wafer (Fig. 1b,c). These wafers were not used directly, but served as templates to produce cell culture materials.

For reproduction of polystyrene (PS) replicates, 0.5 g PS dissolved in 3 mL chloroform was cast onto a 4'' silicon wafer and the chloroform was evaporated overnight. PS rings (2.0 cm Ø for adhesion analysis, 3.0 cm Ø for time lapse CLSM, and 4 cm Ø for AFM adhesion measurements) were glued to substrates using a small amount of casting solution to create cell culture dishes. Substrates received a radiofrequency glow-discharge (RFGD; Harrick, Ithaca, NY, USA) treatment for 5 min in argon gas at 10^{-2} bar for sterilisation and to improve wettability. The groove dimensions of the different nanopatterns were routinely verified by AFM.

AFM imaging

A multimode AFM (Nanoscope IIIa, Veeco, Santa Barbara, CA, USA) with NanoScope Analysis software (version 1.20, Veeco) was used to confirm surface topography of the nanopatterned replicas. Tapping in ambient air was performed with high aspect ratio NW-AR5T-NHCR cantilevers (NanoWorld AG, Wetzlar, Germany) with average nominal spring constants of 30 Nm^{-1} (Loesberg *et al.*, 2007). Height images of each nanopattern were captured in ambient air at 50 % humidity at a tapping frequency of ~250 kHz. The analysed field was scanned at a rate of 0.8 Hz with 512 scanning lines.

Cell culture

The mouse MC3T3-E1 osteoblast cell line (ATCC #CRL-2593) was maintained in alpha Minimal Essential Medium without ascorbic acid (αMEM; Gibco BRL, Life Technologies, Breda, The Netherlands) supplemented with 10 % foetal calf serum (FCS; Gibco) and 0.5 mg/mL gentamicin (Gibco). Cells were cultured from passage 21 up to 25. Before the experiments, cells were detached with trypsin/EDTA (0.25 % w/v trypsin / 0.02 % EDTA), resuspended in cell culture medium, centrifuged at 1,200 rpm for 5 min, and again resuspended at the desired cell density.

For experiments under serum-reduced or serum-free conditions, cells were washed once in phosphate-buffered saline (PBS) after spinning down the cells at 1,200 rpm, centrifuged again at 1,200 rpm and resuspended in serum-reduced or serum-free αMEM.

a

Pitch	Ridge (nm±SE)	Groove (nm±SE)	Depth (nm±SE)
1000 nm	536 ± 10	453 ± 18	158 ± 10
600 nm	320 ± 16	305 ± 8	143± 10
300 nm	175 ± 5	130 ± 8	70 ± 8
200 nm	82 ± 3	135 ± 3	52 ± 3
150 nm	72 ± 6	77 ± 6	33 ± 2

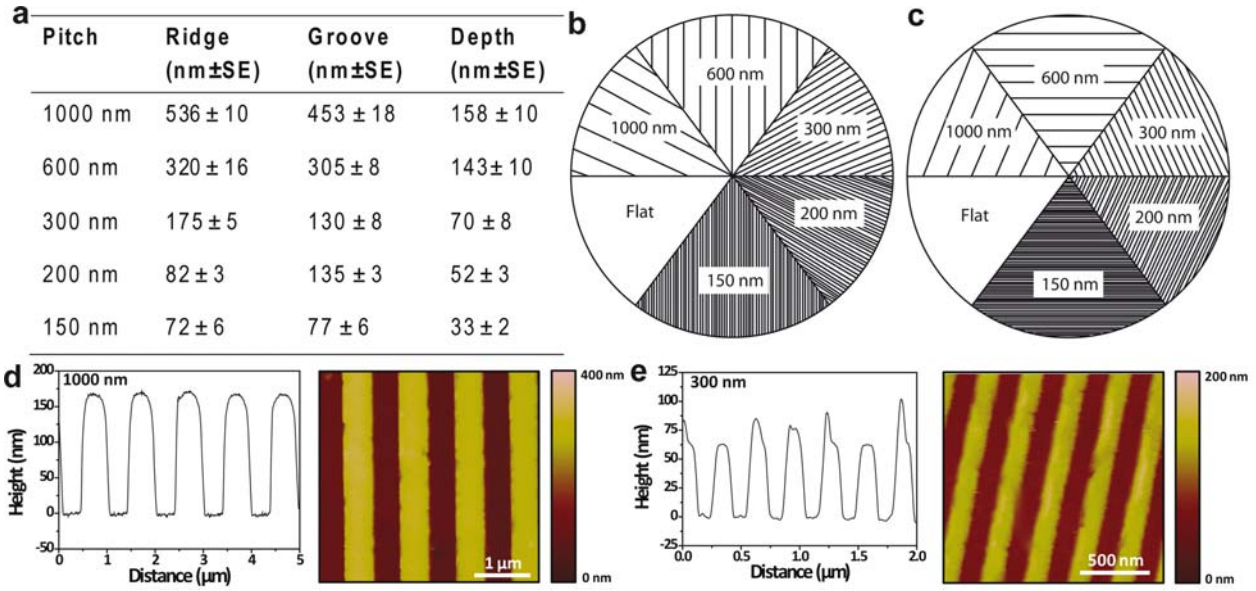

Fig. 1. a. Groove dimensions ± standard error of the mean. **b, c.** Schematic diagram of multi-patterned substrates. **d, e.** Cross-sections and height images of the nanopatterns created by AFM imaging.

AFM force measurements

Cells were attached to tipless AFM cantilevers (MLCT-O10, Bruker, Santa Barbara, CA, USA) by concanavalin A (ConA)-mediated linkages as described (Friedrichs *et al*., 2010; te Riet *et al*., 2007; Wojcikiewicz *et al*., 2003). In short, ConA-coated cantilevers were prepared as follows. Cantilevers were first cleaned by immersion in 1 M sulphuric acid (Sigma-Aldrich, Zwijndrecht, The Netherlands) for 1 h, then thoroughly rinsed with Milli-Q water, ethanol, and subsequently dried in a N_2-flow. Following an overnight incubation at 4 °C in biotinylated BSA (biotin-BSA, 0.5 mg/mL in 100 mM $NaHCO_3$, pH 8.6) the cantilevers were rinsed using PBS and exposed to 0.5 mg/mL streptavidin (Pierce, Rockford, IL, USA) in PBS for 30 min at 37 °C. Finally, the cantilevers were rinsed three times with 20 mM Tris, 150 mM NaCl, 1 mM $CaCl_2$, 2 mM $MgCl_2$, pH 8.0 (TSM) and incubated in biotinylated ConA (biotin-ConA, 0.4 mg/mL in TSM) for 30 min at 37 °C, then washed with TSM. Force measurements on living cells were performed in force-distance mode using a combined Catalyst BioScope AFM (Bruker) Leica confocal microscope TCS SP5 II (Leica, Mannheim, Germany). Cantilever deflection was determined from the difference in signal generated by a two-segment photodiode monitoring the reflection of a laser beam focused onto the apex of the cantilever. The spring constant of each cantilever was calibrated before use by a non-destructive thermal oscillation method (te Riet *et al*., 2011).

For AFM cell adhesion measurements ($n \geq 7$ cells), a cell was first adhered to the cantilever. The cantilever was pushed softly (< 5 nN) onto the cell for approximately 20 s and upon retraction a positive pick up was directly observed by the microscope (Fig. 2a). From that moment, the cell was allowed to adhere strongly to the cantilever for at least 15 min. Adhesion of the cell adhered to the cantilever to the different nanostructures was subsequently measured by bringing the cell into contact with the substrate with a contact force of 1000 pN and allowing the cell to adhere for 10 s. Subsequently, the cell was retracted at a retraction speed at 12 µm/s, with subsequently a relaxing time of 2 s to give the cell time to recover (Fig. 2b) (Friedrichs *et al*., 2010; Weder *et al*., 2009). Cell adhesion experiments were performed in either 10 % serum, 1 % serum, or in serum-free conditions. Data were subsequently exported from the BioScope Catalyst by the NanoScope v8.1 software and further analysed in MATLAB in custom written software. Analysis of force-distance curves resulted in the width, work, and maximum detachment force F_{max} of every curve (see also Fig. 2c) for statistical analysis ($n \geq 70$ curves).

RGD control

AFM force measurements were first performed with a cell in 1 % serum on grooves with a 600 nm and 1000 nm pitch. Cells were then incubated for 30 min with 250 µM RGD peptide (G1269, Sigma-Aldrich). Subsequently, force measurements were repeated in the presence of the peptide ($n \geq 40$ curves; $n = 3$ cells).

Cell adhesion analysis

Cells were seeded at a cell density of 12,500 cells/cm^2 on flat substrates with either 10 % FCS, 1 % FCS, or without FCS ($n \geq 10$). On grooved substrates, 10 % FCS was always used. After allowing the cells to adhere for either 15, 30 or 60 min, the culture medium containing non-adhered cells was transferred into tubes. Cells in the culture medium were spun down at 1,200 rpm for 5 min, medium was removed, and 0.5 mL Milli-Q water was added in order to lyse the cells. In addition, the substrates were washed in PBS to remove medium and serum components, then 0.5 mL Milli-Q water was added, rinsed, and the cells were transferred into separate tubes. Finally, cells were lysed in a series of three freeze-thaw cycles. Subsequently, DNA

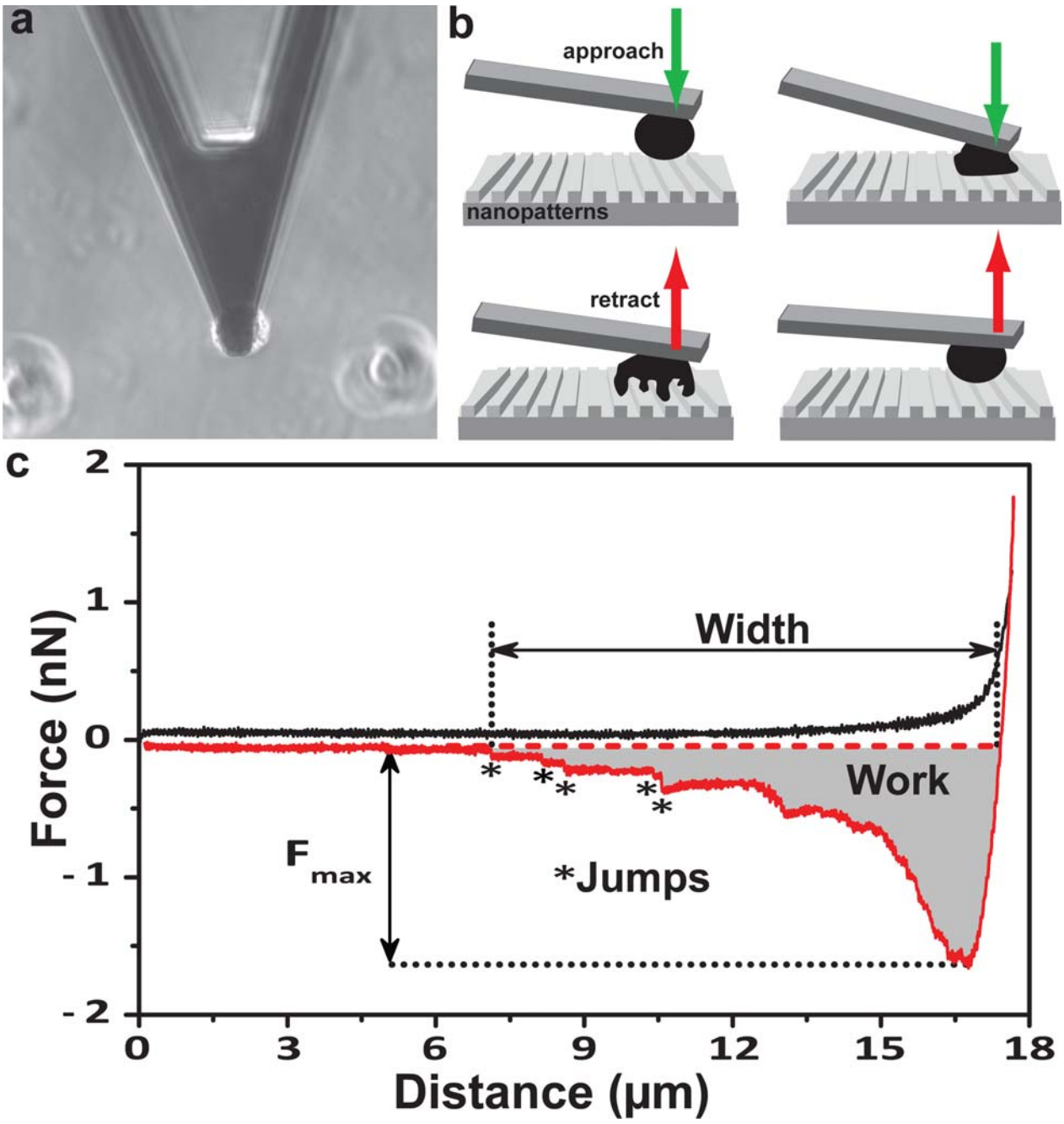

Fig. 2. a. Image of osteoblast adhered to the cantilever above the substrate (cells on substrate are out-of-focus). **b.** Schematic overview of AFM-based single cell adhesion experiments. The cell-functionalised cantilever was approached towards the surface (I). The cell was allowed to adhere for 10 s to the substrate (II). The cell-functionalised cantilever was then retracted from the substrate thereby disrupting adhesion bonds (III) until the cell was completely detached (IV) and a probing cycle can be repeated. **c.** Example of a force-distance curve showing maximum detachment force (F_{max}), the width of detachment, the detachment work, and a number of detachment events of single tethers (jumps, indicated by *).

was separated from the cell remnants by centrifugation at 1,200 rpm for 5 min. The amount of DNA was quantified using the picogreen DNA assay (Invitrogen, Paisley, UK), according to manufacturer's protocol. Briefly, 100 µL of sample was added to 100 µL freshly prepared working solution containing picogreen in a 96-well plate (Greiner Bio-one, Alphen a/d Rijn, The Netherlands) and incubated for 5 min in the dark. The plate was read in a multiplate fluorescence reader at a wavelength of 488 nm. Cell adhesion was analysed by dividing the adhered DNA fraction from the total DNA amount (i.e. sum of DNA from adhered and non-adhered cells).

Preferential migration

Preferential osteoblast migration on nanogrooves was determined ($n \geq 7$) using a multipatterned substrate. Cells were seeded in the substrate centre in a drop of 10 µL containing 5,000 cells for two hours for adherence. Then 1

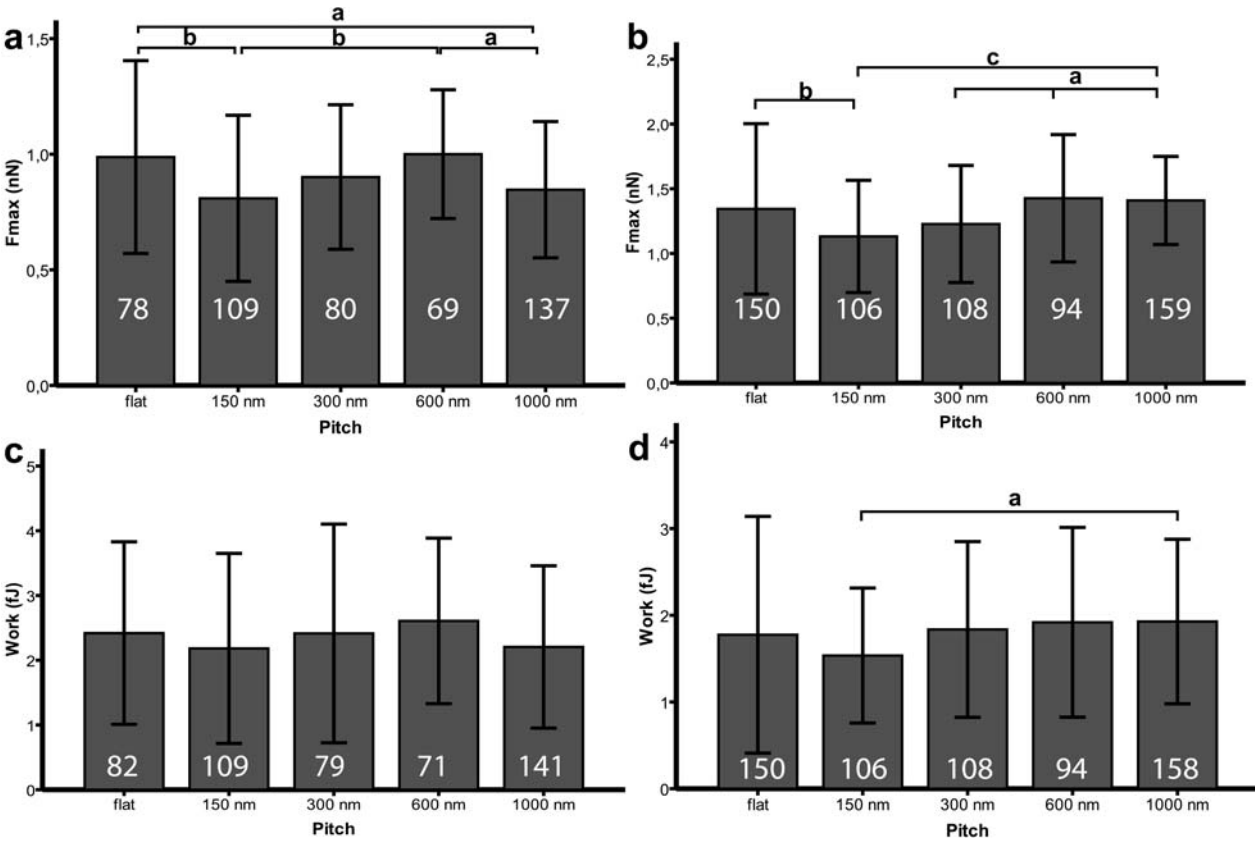

Fig. 3. Detachment of single osteoblasts from nanogrooved substrates in the presence of 1 % FCS (**a, c**) or 10 % FCS (**b, d**). **a, b.** Maximum detachment forces in nN (F_{max}). **c, d.** Work of cellular detachment in femtojoules (fJ). Data represent the mean ± standard deviation. $n > 7$ cells, $n > 10$ force curves per cell, and $n > 3$ locations per cell. Total number of measurements are indicated in the boxes. Data sets were compared by using the ANOVA and *post hoc* Tukey testing. [a] $P < 0.05$, [b] $P < 0.01$, [c] $P < 0.001$.

mL medium was added over the whole substrate and cells were cultured for 3 d. Subsequently, cells were fixed in 3 % paraformaldehyde (Sigma-Aldrich) supplemented with 0.01 % glutaraldehyde (Acros, Geel, Belgium) in PBS, and incubated in PBS with 1 % triton X100 (Koch, Colnbrook, England) for 10 min. The cells were fluorescently labelled with phalloidin-Alexa 568 (1:250; Molecular Probes, Invitrogen) for filamentous (F-) actin and DAPI (1:2500) for nuclear staining in PBS supplemented with 0.1 % Tween 20 (Merck, Schuchardt, Germany). Cells were imaged with a Zeiss Z1 microscope (Jena, Germany) and outward osteoblast migration was determined by Fiji software (Version 1.45b, NIH, La Jolla, USA). The migration analysis demonstrated that the migration distances of cells on the substrates were very different (range between 3 and 6 mm out-growth). Therefore, data was ranked to determine the relative migration effect of grooves on the cells with the following parameters: 1: minimal outward migration and 6: maximal outward migration.

Statistical analysis

For the AFM force measurements, several force-distance curves were acquired per cell on the tested substrate, showing no clear trends and a normal distribution, as was analysed with a Kolmogorov-Smirnov test. Possible autocorrelation effects were analysed with a Durbin-Watson test. Measurements performed on the same location gave similar force curves, indicating that the RGD-protein-containing serum proteins were firmly attached to the surface. Data from the AFM measurements were normalised to the results from the 1000 nm patterns. Data obtained from the experiments were statistically analysed using SPSS for Windows (SPSS 16). Data were analysed by ANOVA and *post hoc* Tukey testing. Probability (P) values of $P \leq 0.05$ were considered significant. Errors are mean ± SD.

Independent T-tests were performed to compare cell adhesion between two groups. Mann-Whitney U-tests were performed to compare cellular migration.

Results

Nanopatterned substrates

AFM analysis of RFGD-treated polystyrene replicates from the multi-patterned wafer confirmed that the replication quality of the groove patterns was consistent throughout the experiments (Fig. 1d,e).

Initial cell adhesion to nanogrooved substrates

In the presence of 1% FCS, cells demonstrated the highest F_{max} on flat and 600 nm pitch substrates and the lowest F_{max}

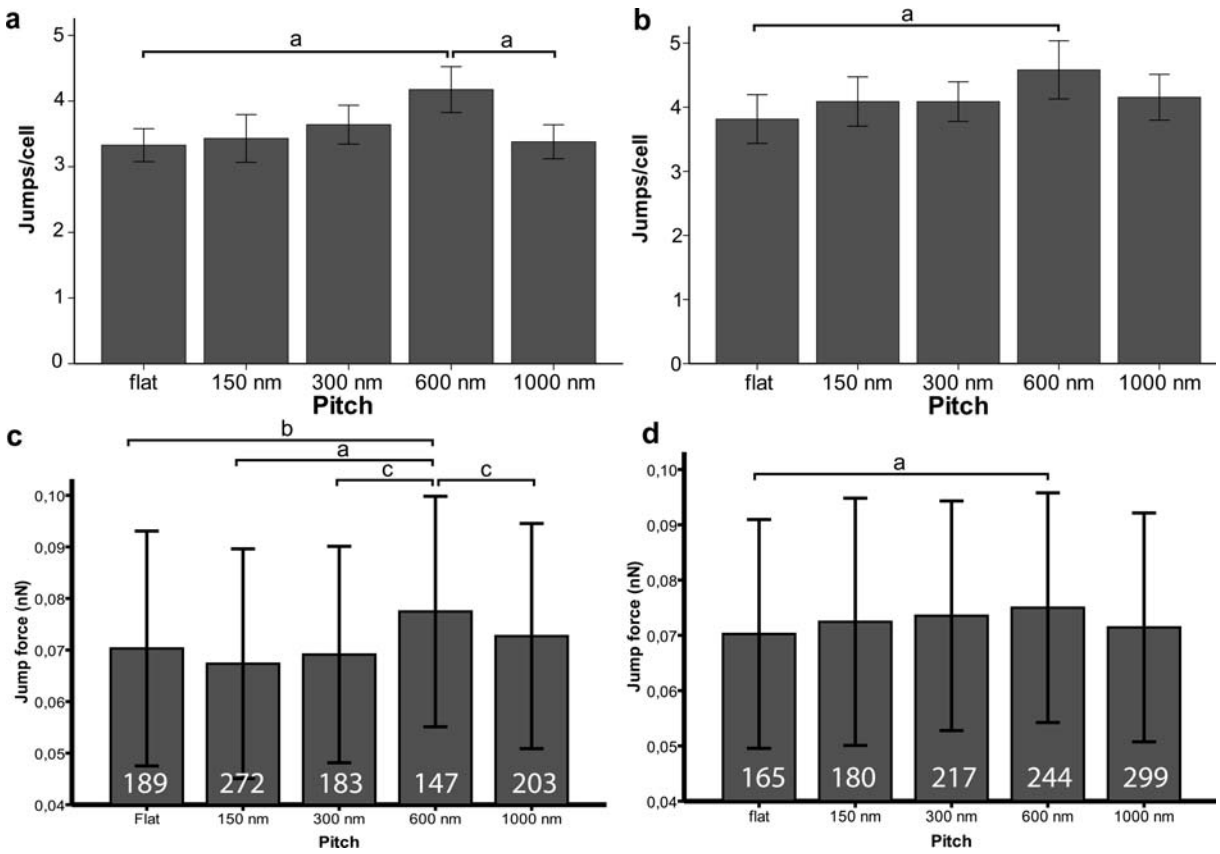

Fig. 4. Number of jumps per cell and jump forces in the presence of 1 % FCS **(a, c)** or 10 % FCS **(b, d)**. **a, b.** Average number of jumps per cell on the nanogrooved substrates. **c, d.** Mean rupture force of each jump. Data from the number of jumps represent the mean ± 95 % confidence interval and from jump forces represent mean ± standard deviation. Total number of measurements are indicated in the boxes. [a] $P < 0.05$, [b] $P < 0.01$, [c] $P < 0.001$.

on a 150 nm substrate (Fig. 3). The "work" (i.e. the area enclosed by the detachment curve and baseline, which gives a measure for the strength of adhesion of the cell to the substrate, Fig. 2c) showed no significant differences. In the presence of 10 % FCS, cells demonstrated the highest F_{max} on 600 nm and 1000 nm pitch substrates and lowest force on a 150 nm pitch. For the work a similar trend was observed; on a 1000 nm pitch the detachment work was significantly higher than on a 150 nm pitch. Comparison of the serum concentration effect on cell adhesion, demonstrated that F_{max} was significantly higher in the presence of 10 % FCS than in 1 % FCS. In contrast, the work was significantly higher in the presence of 1 % FCS than with 10 % FCS.

In the force-distance curves of detaching osteoblasts, step-like unbinding events ("jumps") were observed preceded by force plateaus directly after the F_{max} detachment peak (Fig. 2c). These events probably represent events of membrane tethers unbinding from the substrate. Most jump-events were observed on a substrate with 600 nm pitch, both in the presence of 1 % and 10 % FCS (Fig. 4). In addition, the highest jump forces were also determined on the 600 nm pitches, both in the presence of 1 % and 10 % FCS. The lowest jump forces were observed on the 300 nm pitch, whereas in the presence of 10 % FCS the lowest forces were observed on a flat substrate. Comparison of serum effects on cellular unbinding events demonstrated that the number of jumps were significantly higher in the presence of 10 % FCS compared to 1 % FCS, and that jump forces were significantly higher in the presence of 1 % FCS than with 10 % FCS.

Addition of the RGD blocking peptide reduced both detachment forces and work significantly, but not completely, indicating that RGD-specific integrins are the main initial adhesive source for the cells (Fig. 5).

Adhesion maturation

A comparison of osteoblast adhesion at 15 min showed that only on a 150 nm pitch significantly more cells adhered relative to the 600 nm pitch and the flat substrate (Fig. 6a). At 30 min, more cells adhered to substrates with a pitch of 300 nm, 600 nm and 1000 nm compared to the flat substrate. At 60 min, no significant differences in cell adhesion between the patterns were observed. It is noticeable that at 60 min more than 90 % of the cells stayed adhered, thus, differences in adhesion could not be detected anymore with high sensitivity.

Addition of different serum concentrations to the cells significantly affected cell adhesion at 15-60 min on flat substrates; cell adhesion under serum free conditions was always higher than in the presence of 1 % or 10 % FCS for all interaction times studied (Fig. 6b).

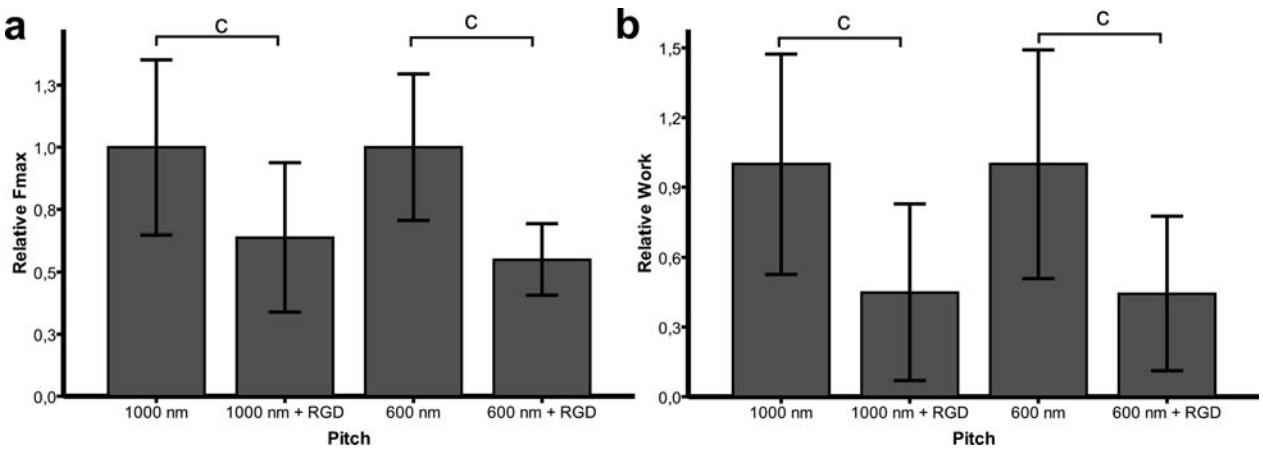

Fig. 5. Effect of 30 minutes block with RGD on cell detachment from a 600 nm and 1000 nm pitch. **a.** Relative maximum detachment forces. **b.** Work of cellular detachment. Data represent the mean ± standard deviation. [a] $P < 0.05$, [b] $P < 0.01$, [c] $P < 0.001$.

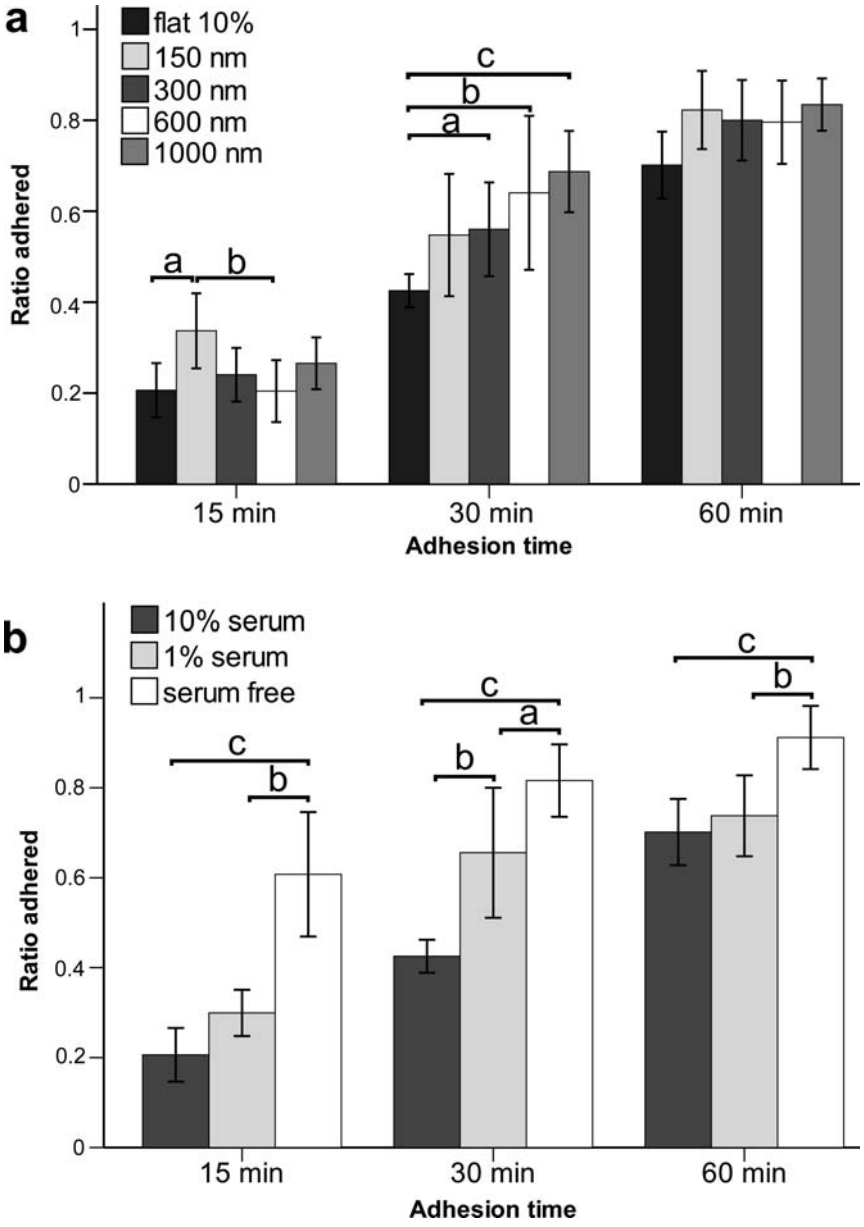

Fig. 6. Quantification of cell adhesion after different adhesion times. **a.** Fraction of adhered cells on different nanogroove dimensions. **b.** Influence of serum concentration on cell adhesion. Data represent the mean ± 95 % confidence interval. [a] $P < 0.05$, [b] $P < 0.01$, [c] $P < 0.001$.

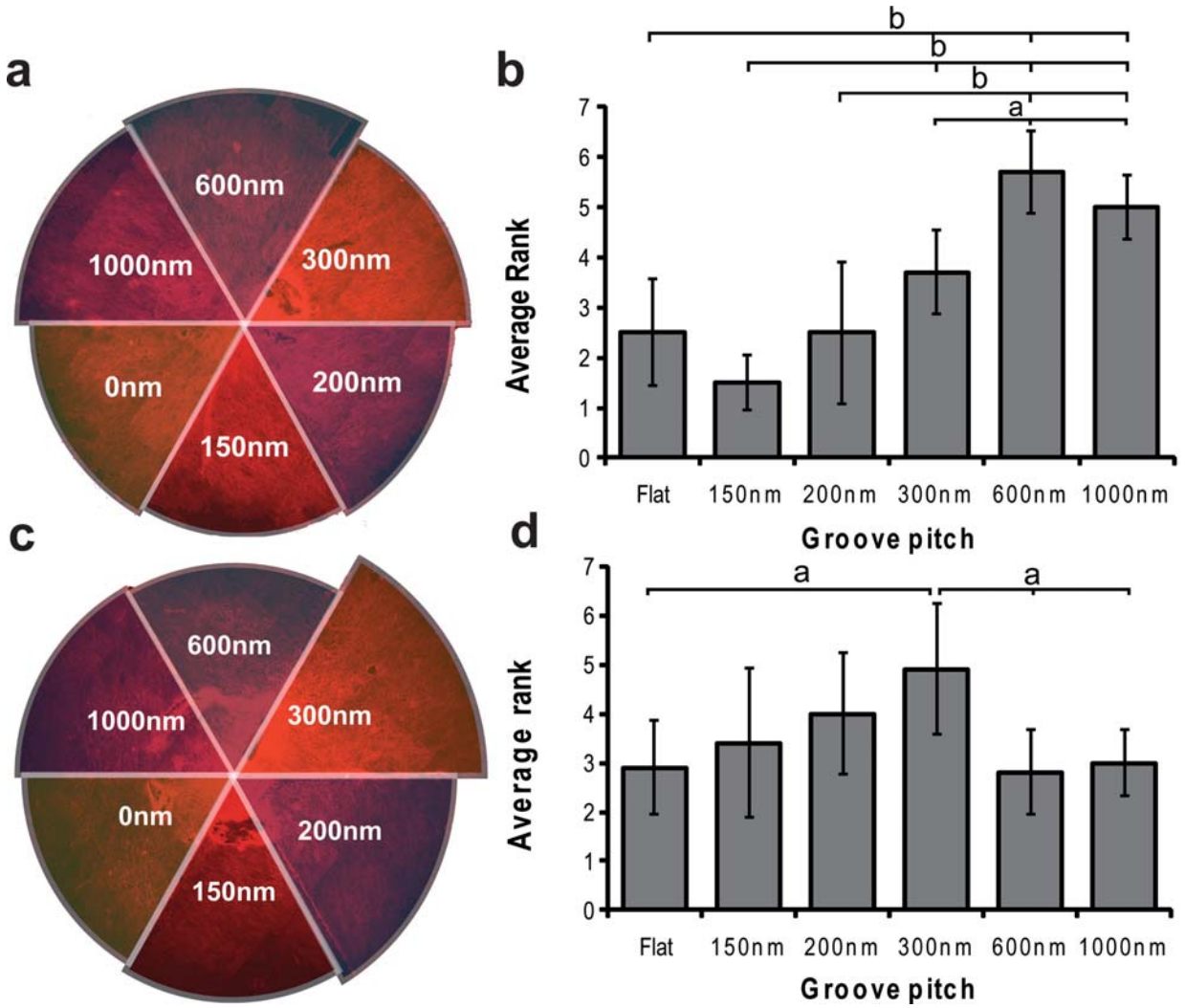

Fig. 7. The influence of nanogrooves on outward migration of osteoblasts. The migration was analysed on radially oriented (**a, b**) or concentrically oriented (**c, d**) grooves. **a, c**. Representative micrographs of outward migration of MC3T3-E1 osteoblasts on the multi-patterned substrates. The size of the sextants are representative for the outgrowth of the cells. **a, c**. Image borders represent migration edges. Data in **b, d** represent the mean ± 95 % confidence interval. [a] $P < 0.05$, [b] $P < 0.01$, [c] $P < 0.001$.

Directional cell migration

Analysis of outward osteoblast migration demonstrated that cells on the radially oriented substrates had the highest outward migration on substrates with a 600 nm pitch and the lowest migration on substrates with a 150 nm pitch (Fig. 7a,b). On the concentrically orientated substrates the highest outward migration was observed on a 300 nm pitch and lowest migration on a 600 nm pitch (Fig. 7c,d).

Discussion

The aim of the current study was to determine the influence of nanoscale grooves on initial adhesion and long-term migration of MC3T3-E1 osteoblasts, using different nanogrooved pitches with a ridge-groove ratio of 1:1 ranging from 150 nm up to 1000 nm and a flat control. The data demonstrated that submicrometer grooves, and most specifically a 600 nm pitch, induce faster initial cell adhesion, whereas at 15 min adhesion on the 600 nm pitch is restrained. AFM-assisted single-cell force spectroscopy (SCFC) proved to be very useful and predictable for standard long-term migration assays. The high initial adhesion and restrained adhesion maturation was favourable to induce a high cell motility and highly directional migration.

Regarding our study from a technical point of view, the use of a multi-patterned substrate had some important advantages over separately patterned substrates. First, replicates of substrates are produced and treated in a single step, and therefore, the variation between substrates due to, for example surface free energy (hydrophobicity), are not potentially significant factors. Secondly, cell migration is instantly comparable within one substrate. Finally, initial cellular adhesion could be studied on different nanopatterns by AFM using a single cell. Thus, statistical comparison in cell assays was free of confounding effects.

Regarding the chosen setup, several techniques can be employed to measure initial cell adhesion. For example,

Modin *et al*. (2006) studied initial osteoblast adhesion by using a quartz crystal microbalance with dissipation (QCM-D). However, this technique is not appropriate to analyse the adhesion strength of single cells. Also, magnetic tweezers have been used to measure forces generated during initial cell adhesion (Walter *et al.*, 2006). A disadvantage of these techniques is their limitation in exerting maximum forces of only ~200 pN, which is mostly not enough to detach the cell. Therefore, another sensitive technique to measure initial cell adhesion forces was used in this study, i.e. AFM-assisted SCFS (Helenius *et al.*, 2008; Muller *et al.*, 2009). A major advantage of SCFS over other techniques is that the adhesion of a cell to a substrate can be very precisely measured over a wide practical force range, from 10 pN to 10^6 pN (Helenius *et al*., 2008). Thereby, SCFS provides insight into adhesion up to single ligand-receptor unbinding of a single cell interaction with a substrate controlling the first moment of contact (Helenius *et al*., 2008; te Riet *et al.*, 2007). Still, the observable step-like dissociation events are probably due to the decoupling of integrin clusters. The technique likely is not sensitive enough for measuring the forces generated in single RGD-fibronectin slip/catch bonds. Thus, our use of the term "membrane tethers" rather than referring to these tethers as a single integrin or focal adhesion bond.

As far as our statistical approach is concerned, it has to be noted that measurements were not calculated per number of cells, but over the total of the curves. This analysis disregards eventual clustering of data within each cell; however is generally accepted as valid (Friedrichs *et al.*, 2010; Puech *et al.* 2005). Previous research states that in this set up, it can be assumed that each of these measurements with the same cell are all different measurements of an interaction of the cell with the substrate. Our analysis of different force-distance curves shows that there is no autocorrelation within the repeated measurements within each cell, and therefore these measurements can indeed be considered as independent measurements (data not shown).

Comparison of our findings with available literature, confirmed again that cells are very sensitive and are able to respond to the smallest variations in topographical characteristics, such as topographical density, organisation and stiffness (Arnold *et al*., 2008; Dalby *et al*., 2007; Kim *et al.*, 2009; Kunzler *et al.*, 2007; Lamers *et al*., 2010a). On the other hand, our comparative study demonstrated for the first time that grooves with a pitch of 600 nm are optimal to induce both nascent cell adhesion and highly directional migration. Moreover, the jump events (representing membrane tether unbinding events) were only significantly increased on a 600 nm pitch. In contrast, a groove pitch of 150 nm reduced nascent adhesion and directional migration. These findings confirm our hypothesis that a sufficient pattern width is essential to promote a fast initial contact of the cell with a substrate, finally resulting in fast and directional migration. Strikingly though, nascent integrin adhesion on nanogrooves is not indicative for the establishment of FBs at later time points. At 15 min, cell adhesion on a 600 nm pitch was reduced, whereas it was enhanced on a 150 nm pitch. Apparently, nascent cell adhesion is promoted by groove widths of 300 nm or larger, whereas the clustering of these integrins into FBs is limited. The maturation of integrin clusters into FBs is indicative for the firmness of adhesion and an increase in FBs reduces cell motility (Zaidel-Bar *et al*., 2003). This possibility fully corroborates with our previous study, in which we demonstrated that upon an increase in groove width up to 300 nm, cell motility increased whereas FA length decreased (Lamers *et al*., 2010b). Veevers-Lowe *et al.* (2011) further confirmed this by demonstrating that cell migration is mediated by integrin adhesion to fibronectin, which in turn induces actin reorganisation and cell migration. In contrast, smaller nanogroove dimensions may be involved in the induction of ECM remodelling rather than cell migration (Ilic *et al.*, 2004). The observation of high initial detachment forces on flat surfaces may be due to adhesive serum proteins such as fibronectin and vitronectin, covering the surface. At longer time points however, cell adhesion to the flat substrate was diminished compared to the grooved substrates, possibly indicating that either a high organisation of adhesive proteins or the topography itself can be essential to establish cell spreading and enhance the formation of mature FAs.

Furthermore, this study demonstrated that cell migration is not only dependent on groove pitch, but also on the direction. The 600 nm pitch induced fast and highly directional cell migration parallel to the grooves, whereas cell migration perpendicular to the 600 nm pitch was highly reduced. In contrast, the 300 nm pitch induced the highest migration perpendicular to the grooves. These findings suggest that there is a threshold for the groove width between 150 nm and 300 nm, above which the formation of mature adhesions perpendicular to the grooves is restrained, resulting in an increasing migration speed and directionality (Fujita *et al.*, 2009). Mature FAs may preferably form in the longitudinal direction along the grooves, resulting in migration parallel to the grooves. On smaller grooves on the other hand, FA formation and maturation may occur perpendicular over several grooves, thereby initiating unidirectional migration (Hamilton *et al.* 2010; Fujita *et al.*, 2009). More importantly though, our cell migration and previously reported motility data (Lamers *et al*., 2010b) fully corroborate with the trend observed in initial cell adhesion, indicating that the initial contact of the cell with a specific surface characteristic may determine the cell fate at later time points (Ayala *et al.*, 2011; Geiger *et al*., 2009). Our previous results on the influence of nanogrooved substrates on osteoblast differentiation confirm this, because differentiation increased with increasing groove pitch (Lamers *et al*., 2010a).

Several groups already demonstrated that differences in serum concentration or type could highly affect cell adhesion (Fujiwara *et al.*, 2009; Grinnell and Feld, 1979; Schmidt *et al.*, 2011). Our study confirmed that serum greatly affects cell adhesion in addition to surface patterning. In the absence of FCS, cells adhered too strongly to the substrate to perform accurate SCFS measurements, and therefore were excluded from the study (data not shown). Serum contains adhesion-mediating proteins, such as fibronectin and vitronectin, which greatly enhance cell adhesion. However, our study demonstrated that cell adhesion was highly increased by decreasing serum concentrations, which corroborates the study by

Fuijwara *et al.* (2009). The extremely high adhesive forces, as observed in the absence of serum, may be resulting from small amounts of adhesive proteins that are secreted by the cells to induce a fast and highly efficient adhesion to the substrate (Grinnell and Feld, 1979). Reduced serum conditions (1 %) also resulted in an increase in cell adhesion compared to high serum conditions (10 %), however in a different manner and to a lesser extent than serum-free conditions. Since we used an MC3T3-E1 osteoblast cell-line, this increase could result from the immortalisation of the cell, however, a similar effect was observed for primary rat MSCs (data not shown). When using a high serum concentration, soluble adhesion proteins present in the culture medium may adhere to integrins on non-adhered cells, thereby reducing cell adhesion to the substrate, which is also loaded with these adhesion proteins. For confirmation, the effect of RGD on cell adhesion was analysed. RGD is a peptide repeat that is present in cell-adhesive proteins such as fibronectin and vitronectin (Humphries *et al*., 2006). Cells recognise the RGD-tripeptide through specific integrins (e.g. β_1, β_3, and β_5 subunits) that reside at the cell surface and are directly linked to the actin filament via the FA-complex. Addition of RGD to the cells resulted in a highly reduced adhesion force and work, indicating that adhesive serum proteins are indeed responsible for integrin-mediated cell adhesion to the substrate, as well as the observed serum effect on initial cell adhesion. For a full confirmation, however, blocking experiments of separate different RGD-sensitive integrins should be performed (Siebers *et al*., 2005).

For clinical applications, finding the optimal surface topographical conditions for cells to adhere, proliferate, migrate, and finally differentiate may greatly enhance the efficacy of implant integration into the surrounding tissue (Biggs *et al*., 2009; McMurray *et al.* 2011). From a cellular point of view, the results from the current study and our previous studies (Lamers *et al.*, 2010a; Lamers *et al.*, 2010b; Lamers *et al.*, 2011a) demonstrate that grooves with a pitch range of 300-1000 nm may be favourable patterns to accomplish such requirements for several reasons: (*i*) Initial cell adhesion, but not adhesion maturation, is enhanced on the 600 nm substrate. Osteoblasts may preferably adhere to such topographies over other cells, thereby reducing possible risks for chronic inflammatory responses by, for example, macrophages or encapsulation by fibroblasts (Kunzler *et al*., 2007; Liu *et al.*, 2010); (*ii*) Cells become highly aligned on substrates with a pitch of 600 nm. Such a realignment may possibly result in a highly ordered ECM deposition around the implant at later time points, leading to an improved stability (Weiner and Wagner, 1998); (*iii*) Directional cell migration parallel to grooves with a 600 nm pitch is increased compared to the other studied substrates. This may result in a faster coverage of the implant surface resembling GTR, thereby improving bone ingrowth and reducing the risk of undesirable side-effects resulting from adhesion of other cells (Stetzer *et al.*, 2002); (*iv*) Osteoblast differentiation is enhanced on substrates with a pitch of 1000 nm (Lamers *et al*., 2010a); (*v*) Moreover, the immune response can be specifically controlled by grooved substrates (Lamers *et al.* 2011a; Refai *et al.* 2004; Wojciak-Stothard *et al.* 1996). These advantages immediately affect the speed of wound closure and bone regeneration. Long term *in vitro* mineralisation studies as well as *in vivo* implantation studies should confirm this hypothesis.

Conclusion

In the current study, we analysed how nanoscale grooves control the adhesion and migration of MC3T3-E1 osteoblasts. The 600 nm pitch (300 nm width) highly induced initial cell adhesion and the formation of integrin to RGD-protein tethers. After 15 min, however, cell adhesion was reduced on a 600 nm pitch. In addition, cell migration parallel to the grooves was highly induced on a 600 nm pitch. From this study, we conclude that grooves with a width of 300 nm may be favourable to enhance adhesion and migration.

Acknowledgement

Confocal laser scanning microscopy and AFM were performed at the microscope imaging centre (MIC) of the Nijmegen Centre for Molecular Life Sciences (NCMLS). This research is supported by the Dutch Science and Technology Foundation STW, applied science division of NWO and the Technology Program of the Ministry of Economic Affairs (project 07621). Joost te Riet is supported by a BIO-LIGHT-TOUCH grant (FP6-2004-NEST-C-1-028781) of the European Union and the Netherlands Institute of Regenerative Medicine (NIRM). The authors thank Michiel Coenen (Dept. of Scanning Probe Microscopy, Radboud University Nijmegen) for helpful advice on programming the software.

References

Arnold M, Hirschfeld-Warneken VC, Lohmuller T, Heil P, Blummel J, Cavalcanti-Adam EA, Lopez-Garcia M, Walther P, Kessler H, Geiger B, Spatz JP (2008) Induction of cell polarization and migration by a gradient of nanoscale variations in adhesive ligand spacing. Nano Letters **8**: 2063-2069.

Ayala R, Zhang C, Yang D, Hwang Y, Aung A, Shroff SS, Arce FT, Lal R, Arya G, Varghese S (2011) Engineering the cell-material interface for controlling stem cell adhesion, migration, and differentiation. Biomaterials **32**: 3700-3711.

Behring J, Junker R, Walboomers XF, Chessnut B, Jansen JA (2008) Toward guided tissue and bone regeneration: morphology, attachment, proliferation, and migration of cells cultured on collagen barrier membranes. A systematic review. Odontology **96**: 1-11.

Biggs MJ, Richards RG, Gadegaard N, Wilkinson CD, Oreffo RO, Dalby MJ (2009) The use of nanoscale topography to modulate the dynamics of adhesion formation in primary osteoblasts and ERK/MAPK signalling in STRO-1+ enriched skeletal stem cells. Biomaterials **30**: 5094-5103.

Carvalho FA, Connell S, Miltenberger-Miltenyi G, Pereira SV, Tavares A, Ariens RAS, Santos NC (2010) Atomic force microscopy-based molecular recognition of a fibrinogen receptor on human erythrocytes. ACS Nano **4**: 4609-4620.

Coussen F, Choquet D, Sheetz MP, Erickson HP (2002) Trimers of the fibronectin cell adhesion domain localize to actin filament bundles and undergo rearward translocation. J Cell Sci **115**: 2581-2590.

Dalby MJ, Gadegaard N, Tare R, Andar A, Riehle MO, Herzyk P, Wilkinson CD, Oreffo RO (2007) The control of human mesenchymal cell differentiation using nanoscale symmetry and disorder. Nat Mater **6**: 997-1003.

Dang JM, Leong KW (2007) Myogenic induction of aligned mesenchymal stem cell sheets by culture on thermally responsive electrospun nanofibers. Adv Mater **19**: 2775-2779.

Friedrichs J, Helenius J, Muller DJ (2010) Quantifying cellular adhesion to extracellular matrix components by single-cell force spectroscopy. Nat Prot **5**: 1353-1361.

Fujita S, Ohshima M, Iwata H (2009) Time-lapse observation of cell alignment on nanogrooved patterns. J Roy Soc, Interface **6 Suppl 3**: S269-S277.

Fujiwara M, Tsukada R, Shioya I, Takagi M (2009) Effects of heat treatment and concentration of fish serum on cell growth in adhesion culture of Chinese hamster ovary cells. Cytotechnology **59**: 135-141.

Gardel ML, Schneider IC, Aratyn-Schaus Y, Waterman CM (2010) Mechanical integration of actin and adhesion dynamics in cell migration. Annu Rev Cell Dev Biol, **26**: 315-333.

Geiger B, Spatz JP, Bershadsky AD (2009) Environmental sensing through focal adhesions. Nat Rev Mol Cell Biol **10**: 21-33.

Grinnell F, Feld MK (1979) Initial adhesion of human fibroblasts in serum-free medium: possible role of secreted fibronectin. Cell **17**: 117-129.

Hamilton DW, Oates CJ, Hasanzadeh A, Mittler S (2010) Migration of periodontal ligament fibroblasts on nanometric topographical patterns: influence of filopodia and focal adhesions on contact guidance. PLoS One **5**: e15129

Helenius J, Heisenberg CP, Gaub HE, Muller DJ (2008) Single-cell force spectroscopy. J Cell Sci **121**: 1785-1791.

Humphries JD, Byron A, Humphries MJ (2006) Integrin ligands at a glance. J Cell Sci **119**: 3901-3903.

Ilic D, Kovacic B, Johkura K, Schlaepfer DD, Tomasevic N, Han Q, Kim JB, Howerton K, Baumbusch C, Ogiwara N, Streblow DN, Nelson JA, Dazin P, Shino Y, Sasaki K, Damsky CH (2004) FAK promotes organization of fibronectin matrix and fibrillar adhesions. J Cell Sci **117**: 177-187.

Kim DH, Han K, Gupta K, Kwon KW, Suh KY, Levchenko A (2009) Mechanosensitivity of fibroblast cell shape and movement to anisotropic substratum topography gradients. Biomaterials **30**: 5433-5444.

Kunzler TP, Drobek T, Schuler M, Spencer ND (2007) Systematic study of osteoblast and fibroblast response to roughness by means of surface-morphology gradients. Biomaterials **28**: 2175-2182.

Lamers E, Frank Walboomers X, Domanski M, Te Riet J, van Delft FC, Luttge R, Winnubst LA, Gardeniers HJ, Jansen JA (2010a) The influence of nanoscale grooved substrates on osteoblast behavior and extracellular matrix deposition. Biomaterials **31**: 3307-3316.

Lamers E, van Horssen R, Te Riet J, van Delft FC, Luttge R, Walboomers XF, Jansen JA (2010b) The influence of nanoscale topographical cues on initial osteoblast morphology and migration. Eur Cells Mater **20**: 329-343.

Lamers E, Walboomers XF, Domanski M, Prodanov L, Melis J, Luttge R, Winnubst L, Anderson JM, Gardeniers HJ, Jansen JA (2011a) *In vitro* and *in vivo* evaluation of the inflammatory response to nanoscale grooved substrates. Nanomedicine, DOI: 10.1016/j.nano.2011.06.013

Liu D, Abdullah CAC, Sear RP, Keddie JL (2010) Cell adhesion on nanopatterned fibronectin substrates. Soft Matter **6**: 5408-5416.

Loesberg WA, Te Riet J, van Delft FC, Schon P, Figdor CG, Speller S, van Loon JJ, Walboomers XF, Jansen JA (2007) The threshold at which substrate nanogroove dimensions may influence fibroblast alignment and adhesion. Biomaterials **28**: 3944-3951.

Luttge R (2009) Massively parallel fabrication of repetitive nanostructures: nanolithography for nanoarrays. J Phys D **42**: 123001.

McMurray RJ, Gadegaard N, Tsimbouri PM, Burgess KV, McNamara LE, Tare R, Murawski K, Kingham E, Oreffo RO, Dalby MJ (2011) Nanoscale surfaces for the long-term maintenance of mesenchymal stem cell phenotype and multipotency. Nat Mater **10**: 637-644.

Modin C, Stranne AL, Foss M, Duch M, Justesen J, Chevallier J, Andersen LK, Hemmersam AG, Pedersen FS, Besenbacher F (2006) QCM-D studies of attachment and differential spreading of pre-osteoblastic cells on Ta and Cr surfaces. Biomaterials **27**: 1346-1354.

Muller DJ, Krieg M, Alsteens D, Dufrene YF (2009) New frontiers in atomic force microscopy: analyzing interactions from single-molecules to cells. Cur Opin Biotechnol **20**: 4-13.

Pierres A, Benoliel AM, Bongrand P (2002) Cell fitting to adhesive surfaces: A prerequisite to firm attachment and subsequent events. Eur Cells Mater **3**: 31-45.

Pierres A, Benoliel AM, Touchard D, Bongrand P (2008) How cells tiptoe on adhesive surfaces before sticking. Biophys J **94**: 4114-4122.

Puech PH, Taubenberger A, Ulrich F, Krieg M, Muller DJ, Heisenberg CP (2005) Measuring cell adhesion forces of primary gastrulating cells from zebrafish using atomic force microscopy. J Cell Sci **118**: 4199-4206.

Refai AK, Textor M, Brunette DM, Waterfield JD (2004) Effect of titanium surface topography on macrophage activation and secretion of proinflammatory cytokines and chemokines. J Biomed Mater Res A **70**: 194-205

Schmidt D, Joyce EJ, Kao WJ (2011) Fetal bovine serum xenoproteins modulate human monocyte adhesion and protein release on biomaterials *in vitro*. Acta Biomater **7**: 515-525.

Siebers MC, ter Brugge PJ, Walboomers XF, Jansen JA (2005) Integrins as linker proteins between osteoblasts and

bone replacing materials. A critical review. Biomaterials **26**: 137-146.

Stetzer K, Cooper G, Gassner R, Kapucu R, Mundell R, Mooney MP (2002) Effects of fixation type and guided tissue regeneration on maxillary osteotomy healing in rabbits. J Oral Maxillo Surg **60**: 427-436.

te Riet J, Zimmerman AW, Cambi A, Joosten B, Speller S, Torensma R, van Leeuwen FN, Figdor CG, de Lange F (2007) Distinct kinetic and mechanical properties govern ALCAM-mediated interactions as shown by single-molecule force spectroscopy. J Cell Sci **120**: 3965-3976.

te Riet J, Katan AJ, Rankl C, Stahl CW, van Buul AM, Phang IY, Gomez-Casado A, Schön P, Gerritsen JW, Cambi A, Rowan AE, Vancso GJ, Jonkheijm P, Huskens J, Oosterkamp TH, Gaub H, Hinterdorfer P, Figdor CG, Speller S (2011) Interlaboratory round robin on cantilever calibration for AFM force spectroscopy. Ultramicroscopy **111**: 1659-1669.

van Soest FJ, van Wolferen HAGM, Hoekstra HJWM, de Ridder RM, Worhoff K, Lambeck PV (2005) Laser interference lithography with highly accurate interferometric alignment. Jap J Appl Phys 1 **44**: 6568-6570.

Veevers-Lowe J, Ball SG, Shuttleworth A, Kielty CM (2011) Mesenchymal stem cell migration is regulated by fibronectin through alpha 5 beta 1-integrin-mediated activation of PDGFR-beta and potentiation of growth factor signals. J Cell Sci **124**: 1288-1300.

Walter N, Selhuber C, Kessler H, Spatz JP (2006) Cellular unbinding forces of initial adhesion processes on nanopatterned surfaces probed with magnetic tweezers. Nano Letters **6**: 398-402.

Weder G, Voros J, Giazzon M, Matthey N, Heinzelmann H, Liley M (2009) Measuring cell adhesion forces during the cell cycle by force spectroscopy. Biointerphases **4**: 27-34.

Weiner S, Wagner HD (1998) The material bone: Structure mechanical function relations. Ann Rev Mater Sci **28**: 271-298.

Wojciak-Stothard B, Curtis A, Monaghan W, MacDonald K, Wilkinson C (1996) Guidance and activation of murine macrophages by nanometric scale topography. Exp Cell Res **223**: 426-435

Wojcikiewicz EP, Zhang X, Chen A, Moy VT (2003) Contributions of molecular binding events and cellular compliance to the modulation of leukocyte adhesion. J Cell Sci **116**: 2531-2539.

Yim EK, Pang SW, Leong KW (2007) Synthetic nanostructures inducing differentiation of human mesenchymal stem cells into neuronal lineage. Exp Cell Res **313**: 1820-1829.

Zaidel-Bar R, Ballestrem C, Kam Z, Geiger B (2003) Early molecular events in the assembly of matrix adhesions at the leading edge of migrating cells. J Cell Sci **116**: 4605-4613.

Discussion with Reviewers

Reviewer I: Would the authors see their AFM method extended to other cell types, such as cells involved in the immune response to implants?

Authors: The AFM method is being applied to study adhesion in many cell types, for example, CHO cells, HUVEC cells, Jurkat cells, etc. A nice overview of cells being studied by single-cell force spectroscopy (SCFS) is given in Table 1 of Helenius *et al*. (2008). Moreover, in a previous study we analysed the effect of nanogrooves on macrophage behaviour and observed that the behaviour is very different from osteoblasts (Lamers *et al.*, 2011a). In this particular study we observed that nanogrooves control the behaviour of the immune response both *in vitro* and *in vivo*. Possibly, the initial adhesion of an immune cell is a determining factor for controlling the immune response.

Reviewer I: Could the authors envisage the AFM method to be applied dynamically in such a way that mechanical stimulation could be measured?
Authors: The versatility of AFM could definitely open up the way to mechanically stimulate cells by nano-manipulation and study responses of cell dynamics, such as envisioned in Helenius *et al.* (2008).

Reviewer II: The authors state that cell adhesion is increased on wider grooves. This may be due to increased surface area as cells are able to interact with the grooves and ridges, while cellular interaction within narrower grooves may be perturbed so reducing cell/substrate contact. Have the authors established which groove widths facilitate cellular infiltration?
Authors: Recently, we analysed the interface interactions between cells and nanogrooved surfaces (Lamers *et al.*, 2011b) by creating cross sections through freshly frozen samples, using a novel technique, cryo DualBeam FIB-SEM. This study demonstrated that cells are able to descend into groove with a width of 150 nm. Thus far we have not been able to analyse whether cells are able to infiltrate into smaller grooves, however this would be very interesting to know as this factor can significantly affect cell adhesion and migration.

Reviewer II: The authors make reference to single tethering events and the recording of such. However, it seems unlikely that the system is suitable to monitor the slipping of single integrin bonds, and the frequency of the jumping events is extremely low. It seems more likely that these observed jumps represent the breaking of adhesion of large microscale cellular regions, such as the leading edge. Please comment.
Authors: These 'unbinding events' are attributed to the unbinding of adhesive units, which could be individual or small aggregates of receptors, e.g. integrins, from the substrate. In these tethering events, adhesive units are pulled away from the cell cortex at the tip of a membrane tether, which could extend over tens of microns. For further reading see, for example, Friedrichs *et al.* (2010).

Reviewer III: The authors state that repeated measurements on the same cell can be considered as "semi"-independent measurements". What precisely does this term mean and how did the authors test their data for independence? It would be of interest to report on the degree of autocorrelation of measures made sequentially on the

same cell to help assess whether the measurements are independent and, if not, are there any trends in the parameters. For example, do the values depend on the number of times a cell has been tested?

Authors: In order to prevent a possible problem of autocorrelation between measurements, we measured the different groove patterns in random order within each cell. Furthermore, several measurements on groove patterns were duplicated in order to confirm the absence of autocorrelation. When changes in detachment forces within these replicates were observed, the measurements were aborted and a new cell was selected for measurements. We performed a Durbin-Watson test to analyse whether the repeated measurements were independent. For force measurements in the presence of 1 % FCS, the Durbin-Watson test demonstrated that repeated measurements were fully independent (even on groove patterns). An analysis of the grooves with each cell separately showed that also the duplicated measurements did not induce any autocorrelation effect. For force measurements in the presence of 10 % FCS, however, the Durbin-Watson test demonstrated that outcomes were dependent on groove pattern. An analysis on the autocorrelation within detachment forces on each groove separately, however, demonstrated that the measurements were fully independent. The difference between the 1 % FCS and 10 % FCS groups can be explained by the differences in adhesion strength between the two groups. In addition, larger differences in adhesion forces between the grooves were observed in the presence of 10 % FCS.

Reviewer III: Could the authors discuss the fact that their methods are such that groove pitch correlates with groove depth. For example the 1000 nm pitch is ≈160 nm deep whereas the 150 nm pitch is only ≈33 nm deep - a five-fold difference. How should readers interpret the data? Are the effects produced by groove pitch or groove depth, or interaction of these two parameters?

Authors: We fully agree with the reviewer that ideally we would like to keep the patterns at a constant depth independent of the pitch, however due to the technical limitations this is currently not possible. In our previous study we demonstrated that groove depth increased linearly with the groove width with an average ratio of approximately 2.5 at a R^2 of 0.96 (Lamers *et al*., 2011a). In this study we used a multipatterned substrate with similar dimensions, and the correlation between groove depth and width is 0.92. In another recently published study we analysed the effect of groove depth on cell behaviour (Lamers *et al*., 2010b) and demonstrated that groove depth indeed affects cell behaviour, however, to a minor extent compared to the groove width.

Reviewer III: The effects on adhesion and migration reported by the authors are modest. Could the authors comment on the likely effects of these nanoscale features on cell behaviour when the cells simultaneously encounter microscale features.

Authors: The reported effects on initial cell adhesion are indeed modest. *In vivo*, tissues and organs have many different cues to which cells respond, both in the micro- and nanoscale, as well as mechanical cues. In the current study the interaction between micro- and nanoscale topographies have not been analysed. However, previously we have performed studies on the effect of cell behaviour on the interaction between nanoscale patterns and mechanical stimulation (Prodanov *et al.*, 2009). The amount of such multifactorial models is growing and the number of these studies will further increase in the future. It would also be very interesting to analyse the combined effects of both patterns on one substrate not only *in vitro*, but also *in vivo*. Supramicrometer structures probably have more influence on the mechanical retention and initial stability on implants. In contrast, currently available literature demonstrates that submicro- or nanoscale topographies have a more significant effect on functional cell behaviour (see for example Lamers *et al*., 2010b and McMurray *et al.*, 2011).

Additional References

Lamers E, Walboomers XF, Domanski M, McKerr G, O'Hagan BM, Barnes CA, Peto L, Luttge R, Winnubst LA, Gardeniers HJ, Jansen JA. (2011b) Cryo dualbeam focused ion beam-scanning electron microscopy to evaluate the interface between cells and nanopatterned scaffolds. Tissue Eng C **17**: 1-7.

Prodanov L, te Riet J, Lamers E, Domanski M, Luttge R, van Loon JJ, Jansen JA, Walboomers XF. (2010) The interaction between nanoscale surface features and mechanical loading and its effect on osteoblast-like cells behavior. Biomaterials **31**: 7758.